Received: 16 November 2019 | Revised: 11 June 2020 | Accepted: 14 June 2020

DOI: 10.1002/mrm.28414

NOTE

Magnetic Resonance in Medicine

A retrospective physiological noise correction method for oscillating steady-state imaging

Amos A. Cao | **Douglas C. Noll**

Department of Biomedical Engineering, University of Michigan, Ann Arbor, Michigan, USA

Correspondence
Amos A. Cao, Functional MRI Laboratory, Department of Biomedical Engineering, University of Michigan, 2360 Bonisteel Blvd, Ann Arbor, MI 48109, USA.
Email: amoscao@umich.edu

Funding information
Supported by National Institute of Biomedical Imaging and Bioengineering (NIBIB) and National Institute of Neurological Disorders and Stroke (NINDS) through grants R01 EB023618 and U01 EB026977

Purpose: Oscillating steady-state imaging (OSSI) is an SNR-efficient steady-state sequence with T_2^* sensitivity suitable for FMRI. Due to the frequency sensitivity of the signal, respiration- and drift-induced field changes can create unwanted signal fluctuations. This study aims to address this issue by developing retrospective signal correction methods that utilize OSSI signal properties to denoise task-based OSSI FMRI experiments.

Methods: A retrospective denoising approach was developed that leverages the unique signal properties of OSSI to perform denoising without a manually specified noise region of interest and works with both voxel timecourses (oscillating steady-state correction [OSSCOR]) or FID timecourses (F-OSSCOR). Simulations were performed to estimate the number of principal components optimal for denoising. In vivo experiments at 3 T field strength were conducted to compare the performance of proposed methods against a standard principal component analysis-based method, measured using mean t score within an region of interest, number of activations, and mean temporal SNR.

Results: Correction using OSSCOR was significantly better than the standard method in all metrics. Correction using F-OSSCOR was not significantly different from the standard method using an equal number of principal components. Increasing the number of OSSCOR principal components decreased activation strength and increased the number of suspected false positives. However, increasing the number of principal components in F-OSSCOR increased activation strength with little to no increase in false activation.

Conclusion: Both OSSCOR and F-OSSCOR substantially reduce physiological noise components and increase temporal SNR, improving the functional results of task-based OSSI functional experiments. F-OSSCOR demonstrates a proof of concept utilization of coil-localized FID signal information for physiological noise correction.

KEYWORDS
steady-state imaging, fMRI, OSSI, physiological noise, retrospective correction

1 | INTRODUCTION

Oscillating steady-state imaging (OSSI) is a sequence that combines balanced gradients with a quadratic RF phase increment to produce a large, oscillating signal.[1] This signal has been shown to exhibit frequency sensitivity, which leads to a T_2^* weighting that is similar to gradient echo, creating the potential for high SNR FMRI acquisitions. Whereas OSSI's frequency sensitivity results in desirable T_2^* weighting, it also increases sensitivity to any temporally varying changes to B_0. Two primary causes of B_0 changes over an FMRI experiment are respiration and scanner drift, which are known to vary throughout the brain spatially.[2-5] The resulting physiological noise is commonly addressed in FMRI using a retrospective method as a postprocessing step. However, OSSI exhibits a complex nonlinear response to frequency changes, making model-based correction methods that use external physiological recordings, such as RETROICOR,[6] poorly suited to correct the OSSI signal. Instead, these nonlinear changes to the OSSI steady state may be addressed using previous data-driven approaches that differentiate physiological noise from functional changes through a spatial or temporal model.[7-10]

To this end, we present a novel data-driven method for retrospective correction method titled *oscillating steady-state correction* (OSSCOR). OSSCOR uses principal components as nuisance regressors, similar to existing component-based methods (ex. CompCor).[8]). However, OSSCOR does not rely on specifying a noise region of interest (ROI) and instead utilizes a unique property of OSSI for which multiple images with different contrasts are acquired for each time point. Results from simulation reveal that signal changes caused by frequency changes are low rank across these images, allowing estimation of physiological noise using principal component analysis. We show that the use of OSSCOR-derived nuisance regressors in a task-based FMRI experiment can significantly reduce physiological noise compared to standard methods, as measured by activated voxels, mean t score, and temporal SNR (tSNR). Finally, we present a variation of our approach deemed FID-based oscillating steady-state correction (*F-OSSCOR*), for which FID timecourses are used to generate nuisance regressors instead of image data. By using FID data instead of image data, physiological noise can be sampled every TR, independently of the slice or volume acquisition rate.

2 | METHODS

2.1 | Image-based physiological noise estimation

During an OSSI FMRI experiment, quadratic phase cycling is used to create a periodically oscillating signal that repeats every n_c TRs, for which n_c is a scan parameter. The n_c signals from each period are then combined into 1 time point, resulting in an FMRI image series with an effective temporal resolution of $TR_{eff} = n_c * TR$. The OSSI signal combination strategy is an effective way to reduce frequency-dependent signal variance in steady state. However, temporally varying frequency due to respiration and scanner drift result in transient disturbances to the steady state, resulting in unwanted signal fluctuations. Herein, we refer to such signal fluctuations caused by both sources as *physiological noise* for simplicity.

The OSSCOR method is a data-driven method like CompCor, adapted to the unique acquisition strategy and features of the OSSI signal. First, OSSCOR seeks to remove physiological noise from the OSSI signal prior to the signal combination step in order to exploit shared information between the magnetization states. This information sharing is accomplished by treating each of the n_c phases in an OSSI cycle as separate image timecourses. We refer to each of these separate timecourses as a *phase timecourse*, such that each voxel will have n_c phase time courses prior to combination.

Formally, we can represent the magnitude of an original OSSI voxel timecourse $m \in \mathbb{R}_+^t$ with t time points as the following matrix:

$$\mathrm{M} = \begin{bmatrix} m(1) & m(2) & \dots & m(n_c) \\ m(n_c+1) & m(n_c+2) & \dots & m(2n_c) \\ \vdots & \vdots & \ddots & \vdots \\ m(t-n_c+1) & m(t-n_c+2) & \dots & m(t) \end{bmatrix}, \quad (1)$$

where each column of $\mathrm{M} \in \mathbb{R}_+^{t/n_c \times n_c}$ is a phase timecourse. Although the n_c time points in each row are acquired sequentially, for the purpose of the noise analysis we assume that they are acquired simultaneously because the acquisition time of each row (~100ms) is considerably faster than respiration or scanner drift-induced signal changes. The signals from each row of $\mathbf{M}$ form 1 time point in the combined timecourse $c \in \mathbb{R}_+^{t/n_c}$:

$$c(i) = \sqrt{\sum_{j=1}^{n_c} \mathrm{M}_{ij}^2}. \quad (2)$$

Each phase timecourse will then exhibit different frequency-dependent physiological artifacts. An example of this can be seen in Figure 1A, where simulated respiration and drift result in different physiological artifacts for each phase timecourse. Figure 1B shows how combining phase timecourses can cause constructive or destructive interference of these physiological artifacts, resulting in signal fluctuations that change in amplitude and shape through time.

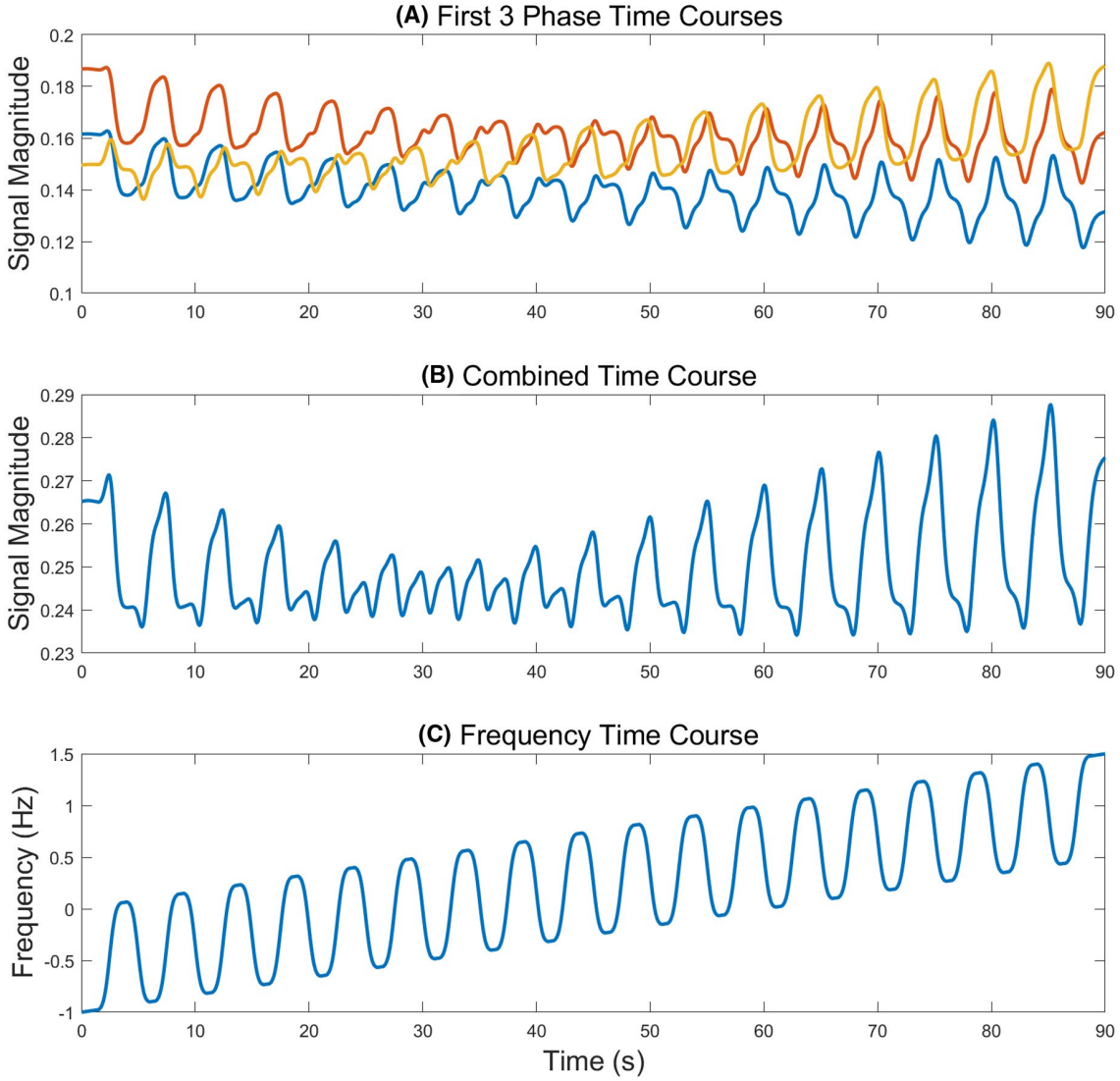

FIGURE 1 Simulated gray matter signals with respiration and scanner drift effects. Plot A shows phase timecourses (3 of 6 plotted for clarity). Plot B shows the associated combined timecourse. Plot C shows simulated B_0 changes modeled using 2 terms: 1) a respiration waveform at 12 breaths/min and peak-to-peak amplitude of 1 Hz, and 2) a linear scanner drift term of 1 Hz/min

We can use the matrix representation of the OSSI signal in Equation (1) to estimate the physiological noise components, which are common between phase time courses and between voxels. We achieve this by forming a block matrix $\mathbf{S}$ for all r voxels:

$$\mathbf{S} = \left[\mathbf{M}_1\, \mathbf{M}_2 \ldots \mathbf{M}_r\right], \tag{3}$$

where the columns of $\mathbf{S}$ are the phase timecourses of all r voxels. Through simulation (as described below), we show that the physiological noise components of $\mathbf{S}$ are low rank and can be represented using principal component analysis (PCA). This is the central concept of OSSCOR; the signal properties of OSSI allow for a small number of principal components to sufficiently describe the physiological noise in any phase timecourse at any spatial location.

Once the principal components of $\mathbf{S}$ are determined, we can remove physiological noise components using the following signal model commonly used for BOLD FMRI:

$$\mathbf{S}_i = \mathbf{X}\beta_1 + \mathbf{T}\beta_2 + \mathbf{P}\beta_3 + \varepsilon, \tag{4}$$

where $\mathbf{S}_i$ is the ith column of $\mathbf{S}$; $\mathbf{X}$ is a matrix of experimental design variables; $\mathbf{T}$ is a matrix of polynomial detrending terms; and $\mathbf{P}$ is a matrix containing principal components of $\mathbf{S}$, which act as nuisance regressors for physiological noise. β_1, β_2, and β_3 contain weights for each respective matrix, and ε is random error. The use of polynomial terms $\mathbf{T}$ was not found to improve the performance of OSSCOR but were

included to maintain consistent degrees of freedom with CompCor in the later comparison.

The number of principal components was determined by simulating OSSI timecourses (TR = 15 ms, flip angle = 10°, $n_c = 6$) with temporally varying B_0. An example of how B_0 was varied can be seen in Figure 1C. The effects of respiration on B_0 were varied by changing the amplitude from 0 to 2 Hz peak to peak, with a step size of 0.1 Hz (21 steps). A center frequency offset was then added to each respiration waveform, for which each respiration waveform was initialized over ±50 Hz with a step size of 0.1 Hz (1001 steps). The respiration rate was kept constant at 12 breaths/min. A linear drift component of 1 Hz/min was added to the respiration component for all frequency amplitude values. T_1 and T_2 were not found to affect the results of the simulation and were held constant at 1286 ms and 110 ms, respectively. Each of the 21,021 parameter combinations was initialized at steady state and simulated for 90 s, then reshaped into a matrix of 126,126 phase timecourses per Equation (1). PCA was then applied to the simulated timecourses. A subsequent scree test was used to select a rank of k = 6 for denoising. Supporting Information Figure S2A shows associated scree plots of the simulated physiological noise.

2.2 | FID-based physiological noise estimation

In addition to image data, principal components can be determined from acquiring extra samples of the signal FID prior to readout. We refer to this as *F-OSSCOR*, a FID-based variation of the previously described method. Although this signal source is not spatially encoded using gradients, the individual coils in a receive array provide spatially varying sensitivity to different regions of the brain, which in turn have varying distributions of off-resonant spins. Similar to a blind source separation problem, PCA can then be used to estimate the independent signals that comprise the low rank physiological noise subspace.

We implement this method by acquiring multiple samples at $k_{xy} = 0$ before readout, which are then averaged into a single magnitude value. This is performed coil-wise, resulting in n_{coil} measurements per TR. Considering these to be n_{coil} separate timecourses, the same methods previously described for image data are then applied. The number of FID samples was varied to determine its effect on the quality of estimates produced, which showed negligible improvement past 16 samples.

2.3 | Experimental setup

All studies ($n = 6$ subjects) were performed on a 3 T GE MR750 scanner (GE Healthcare, Waukesha, WI) with a 32-channel head coil (Nova Medical, Wilmington, MA). All experiments were conducted in accordance with the local institutional review board, and all subjects were provided written informed consent. We implemented the OSSI pulse sequence using the vendor's pulse programming language, EPIC, as well as our own in-house pulse sequence development framework, TOPPE.[11] Single-slice imaging with was performed using a single-shot constant-density spiral-out trajectory ($n_c = 6$, TR = 17.5 ms, flip angle = 10°, FOV = 19 × 19 cm^2, matrix = 45 × 45 reconstructed at 64 × 64, slice thickness = 2.5 mm, sampling BW = 250 kHz), with 16 extra k-space center samples prior to readout. Spatial distortions due to B_0 field inhomogeneity were corrected using a separately acquired field map.

Subjects were presented with a visual stimulus composed of right- and left-hemifield counter-phased 10Hz flickering checkerboards in 40 s blocks, repeated 6 times (240 s). The subject was instructed to gaze at a fixation cross in the center of their visual field during the experiment.

2.4 | Data analysis

Analysis of functional data was performed using MATLAB 2019a (Mathworks, Natick, MA). A block diagram illustrating the following analysis workflow is shown in Figure 2. The OSSCOR and F-OSSCOR analysis methods were applied by removing physiological noise components to phase timecourses **S** using least-squares fitting of the signal model (Equation 4), which included the task waveform and linear/quadratic detrending terms. Six principal components were used in the OSSCOR and F-OSSCOR analyses. The denoised phase timecourses were then combined using Equation (2), resulting in 1 denoised combined timecourse per voxel. For comparison, CompCor was implemented on combined timecourses with linear/quadratic detrending. Temporal SD (tSD) was used to select the top 2% of noisy voxels, discarding any timecourse with task correlation higher than 0.2 (tCompCor variation). In all methods, the resulting denoised combined timecourses were then evaluated for activation using a simple correlation threshold of $r > 0.5$. No high-pass filtering or spatial smoothing was performed.

Method performance was evaluated using average t score, number of activated voxels, and average tSNR. Average t score was calculated within a per-subject ROI defined by the union of the activated voxels found in all correction methods, with $df = 2079$ for each voxel. In counting the total number of activations, only voxels from the bottom-third of the brain could be considered true active, approximately corresponding to the visual cortex. Additionally, because the visual stimulus was counter-phased, only negative correlations were considered from the left hemisphere and positive correlations from the right hemisphere. For comparison, an additional

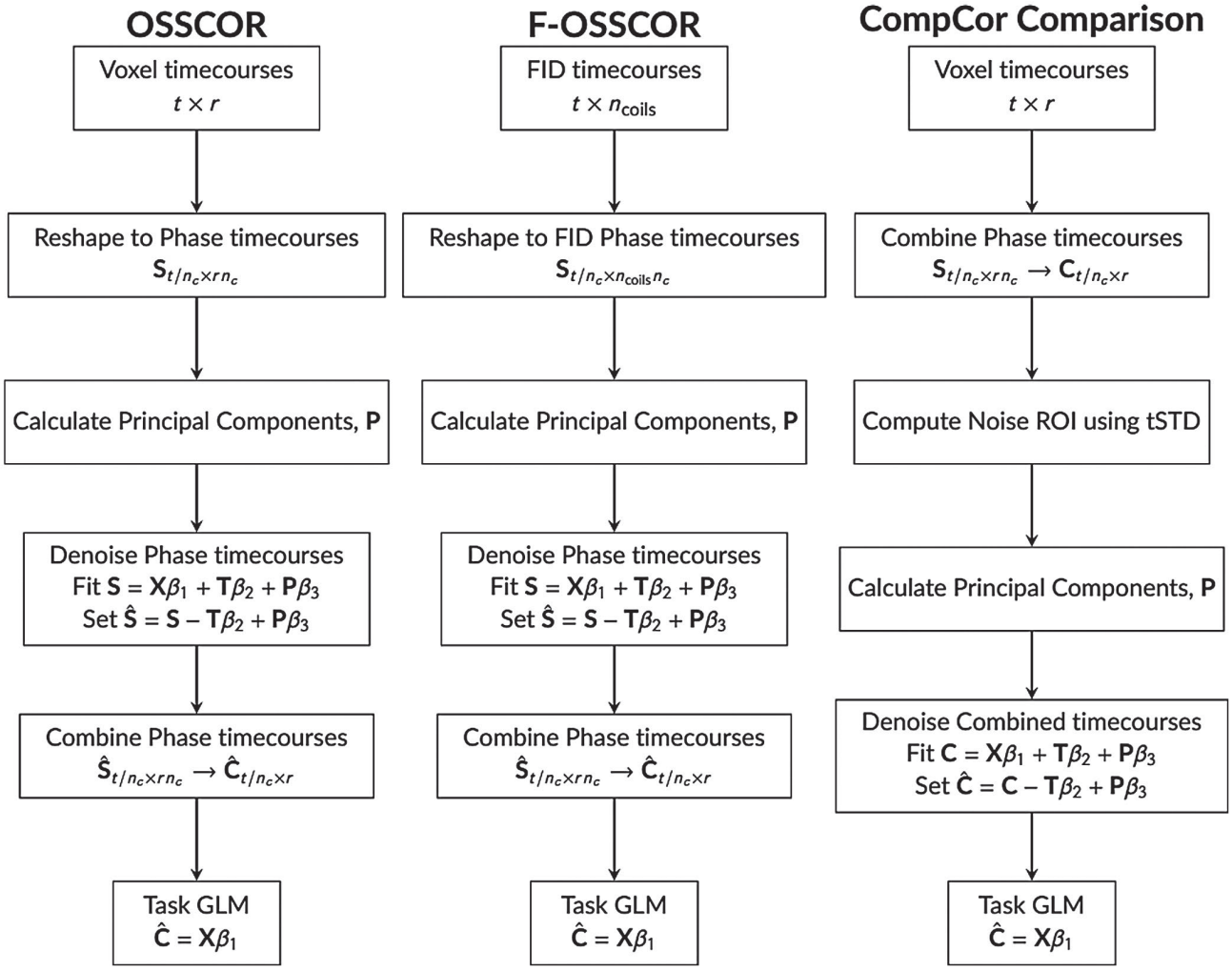

FIGURE 2 A diagram outlining the steps implemented for each analysis method. OSSCOR and F-OSSCOR both calculate principal components and perform denoising before phase timecourse combination, whereas CompCor was applied on the final combined timecourse. CompCor, component-based method; F-OSSCOR, FID-based oscillating steady-state correction; OSSCOR, oscillating steady-state corrrection

nonparametric analysis was conducted using a random blockwise permutation approach with randomized circular shifting, 1 million permutations, and 10 blocks.[12]

3 | RESULTS

Detailed results from 1 subject (no. 4) are described here, with results for other subjects summarized in Table 1. Figure 3A shows activation and tSNR maps for the proposed methods, with CompCor for comparison. Using a paired t test, OSSCOR, F-OSSCOR, and CompCor all significantly improved the number of activated voxels (all $P < .03$, $d > 1.26$), average t score (all $P < .001$, $d > 4.44$), and tSNR (all $P < .001$, $d > 6.36$) compared to only polynomial detrending (Table 1). OSSCOR performed significantly better than CompCor in all 3 metrics ($P = .025$, $P = .042$, $P = .0025$; and $d = 1.29$, $d = 1.11$, $d = 2.29$, respectively). F-OSSCOR results were not found to be significantly different compared to CompCor. An example uncorrected and OSSCOR corrected phase timecourse is shown in Figure 4, illustrating successful reduction of high-frequency respiratory noise as well as drift-induced low-frequency components. The OSSCOR nuisance regressors for subject 4 are shown in Supporting Information Figure S1.

Increasing the number of principal components used in OSSCOR resulted in decreased activation area and mean t score, as well as an increase in false positives as defined by activations outside of the visual task ROI. This reduction of performance was observed across all subjects. However, increasing the rank of the F-OSSCOR analysis improved the number of activations and mean t score across all subjects, with little to no increase in false activation. Activation maps for representative principal component numbers are shown in Figure 3B. Scree plots for OSSCOR and F-OSSCOR are shown in the Supporting Information Figure S2B,C. The results of the random blockwise permutation analysis are shown in Supporting Information Figure S3 and Supporting

TABLE 1 Summary of functional experimental results

	Subject 1	Subject 2	Subject 3	Subject 4	Subject 5	Subject 6
Average t score with detrending	15.1	26.4	38.3	19.0	19.2	27.5
Average t score with CompCor	31.6	43.4	47.0	33.5	31.1	41.7
Average t score with OSSCOR	34.5	44.3	49.4	38.6	41.5	43.2
Average t score with F-OSSCOR	32.8	43.9	48.1	35.7	36.6	41.4
No. activated voxels with detrending	0	16	53	27	10	39
No. activated voxels with CompCor	22	32	66	91	19	67
No. activated voxels with OSSCOR	30	31	71	109	34	75
No. activated voxels with F-OSSCOR	28	28	70	87	27	63
Average tSNR with detrending	47.9	41.4	83.9	60.2	46.1	67.2
Average tSNR with CompCor	88.1	72.0	125.6	94.0	74.1	106.4
Average tSNR with OSSCOR	94.9	94.3	135.9	106.1	83.5	119.2
Average tSNR with F-OSSCOR	87.3	75.9	132.6	95.1	80.4	106.7

CompCor, component-based method; F-OSSCOR, FID-based oscillating steady-state correction; OSSCOR, oscillating steady-state correction; tSNR, temporal SNR.

Information Table S1, showing general agreement with the performance results from the correlation analysis.

4 | DISCUSSION

The *phase timecourse* analysis of OSSCOR assumes that the time to acquire each period of n_c TRs is much shorter than the timescales at which respiration and drift occur. Therefore, temporally varying frequency and resulting transient effects can be treated as quasi-static over the duration of a full n_c OSSI period. This assumption does not imply that transient effects are negligible but rather are slowly varying compared to the speed to acquire a period, TR_{eff}. This assumption performs well at the chosen parameters ($n_c = 6$, $TR_{eff} = 105$ ms), although we found in initial tests that longer readouts or higher n_c values reduced the effectiveness of OSSCOR. Furthermore, higher values of n_c result in reduced amplitude of respiration and drift artifacts due to a more stable combined frequency response, reducing the need for retrospective correction. For example, a period of $n_c = 10$ was shown to have a combined frequency response variation of less than 5% compared to the 17% variation of $n_c = 6$, although at the cost of a 66% longer TR_{eff}.

F-OSSCOR extends the OSSCOR method by using FID timecourses instead of voxel timecourses. Although not spatially encoded, the FID time series data can be used to estimate spatially varying physiological noise due to 2 sources of signal diversity: coil sensitivity and B_0 inhomogeneity. Because the FID signal is detected independently per coil, each coil will only be sensitive to a spatially localized distribution of off-resonant spins with certain physiological noise structure. Furthermore, OSSI effectively acquires a sequence of n_c different images with different center frequencies, resulting in each coil receiving FID signals from n_c different regions of the frequency response. In our experimental setup using a 32-channel head array and $n_c = 6$, the 192 separate FID timecourses produced for the F-OSSCOR analysis were sufficient for correcting the data. An additional benefit of the F-OSSCOR approach is that the requisite FID signals are measured every TR regardless of the encoding strategy and are therefore compatible with any multishot, 3D, or undersampling scheme.

The concept of using FID-based nuisance regressors assumes that FID signal variance is dominated by respiration or drift artifacts that are of lower rank than functional signal changes. This is supported by the comparison shown in Figure 3B, which shows OSSCOR and F-OSSCOR activation maps

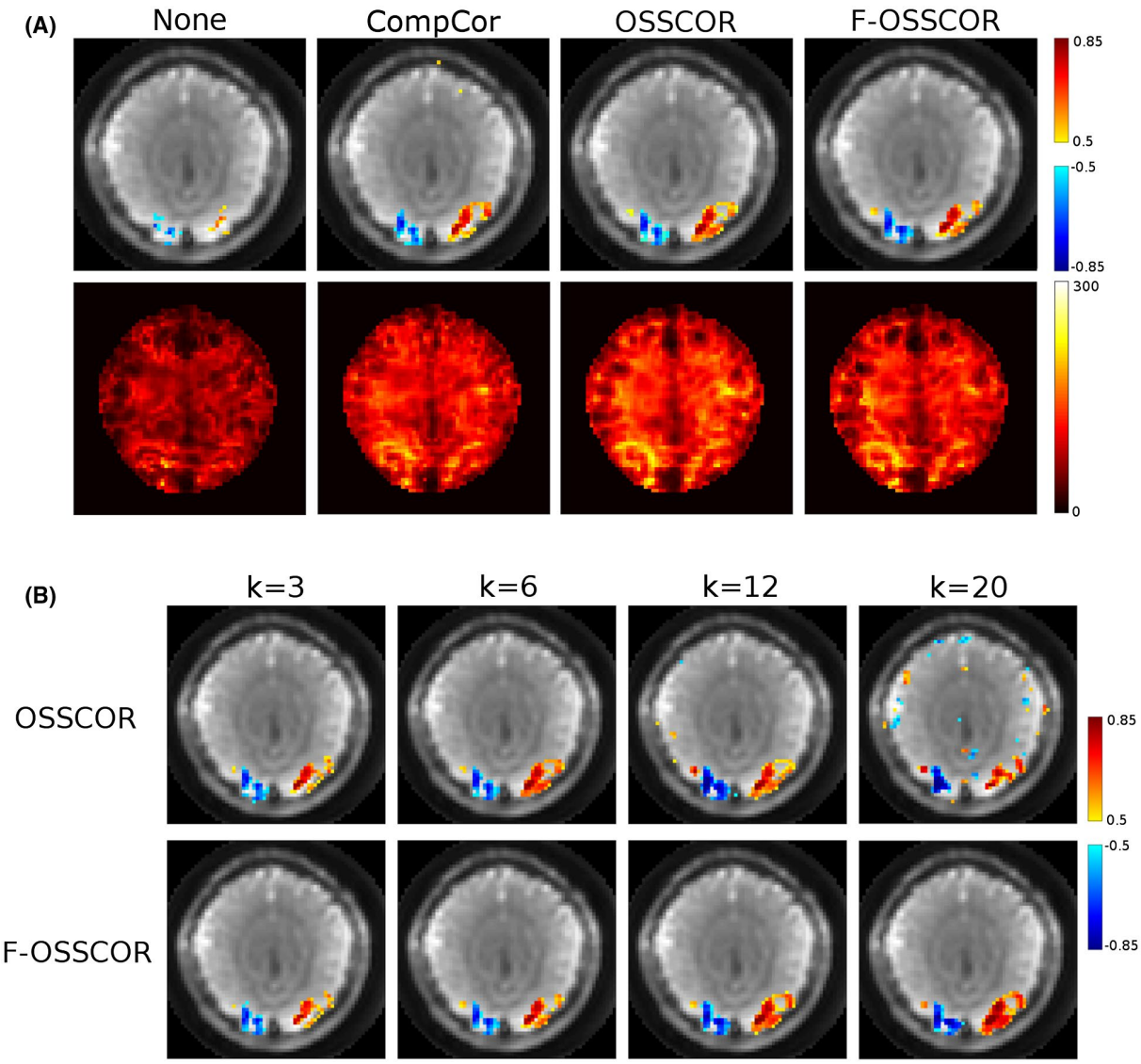

FIGURE 3 (A) Activation and tSNR map for each respective correction methods: polynomial detrending only; and CompCor, OSSCOR, and F-OSSCOR with 6 PCs each. OSSCOR outperformed both CompCor and F-OSSCOR, but all 3 correction methods significantly increased the number of activated voxels and mean tSNR. Voxels with a significant vascular component were observed to have lower tSNR than their surroundings, which is thought to be the effect of through-plane flow unable to reach steady state due to the single-slice acquisition. (B) Activation maps for OSSCOR and F-OSSCOR with varying number of PCs. Increasing the number of OSSCOR PCs reduced activation sensitivity and increased the number of false positives, whereas increasing the number of F-OSSCOR PCs increased sensitivity without increasing false positives. PCs, principal components; tSNR, temporal SNR

denoised using different numbers of principal components. As the number of principal components was increased past the theorized rank of the physiological noise, OSSCOR functional sensitivity and specificity decreased in all subjects. In contrast, increasing the number of principal components in F-OSSCOR increased activation strength with minimal reduction in specificity across subjects while maintaining similar activation areas. We conclude that OSSCOR is more sensitive to the number of PCs used and begins to capture functional activity in its regressors when the selected rank is too high. Conversely, F-OSSCOR performance is relatively insensitive to exceeding the rank of the physiological noise.

Both OSSCOR and F-OSSCOR use PCA to produce nuisance regressors for subsequent functional analysis, similar to the CompCor denoising approach. However, a fundamental difference is that CompCor seeks to target noisy voxels and exclude activated voxels from the PCA by specifying a noise ROI, whereas OSSCOR and F-OSSCOR include all data. Despite including activated voxels in the PCA analysis, OSSCOR performed significantly better than CompCor in all 3 metrics, and F-OSSCOR performed comparably to CompCor. In fact, our testing showed that including all voxels as inputs was found to be critical for OSSCOR because excluding voxels via a tSD threshold resulted in a loss of denoising performance. This

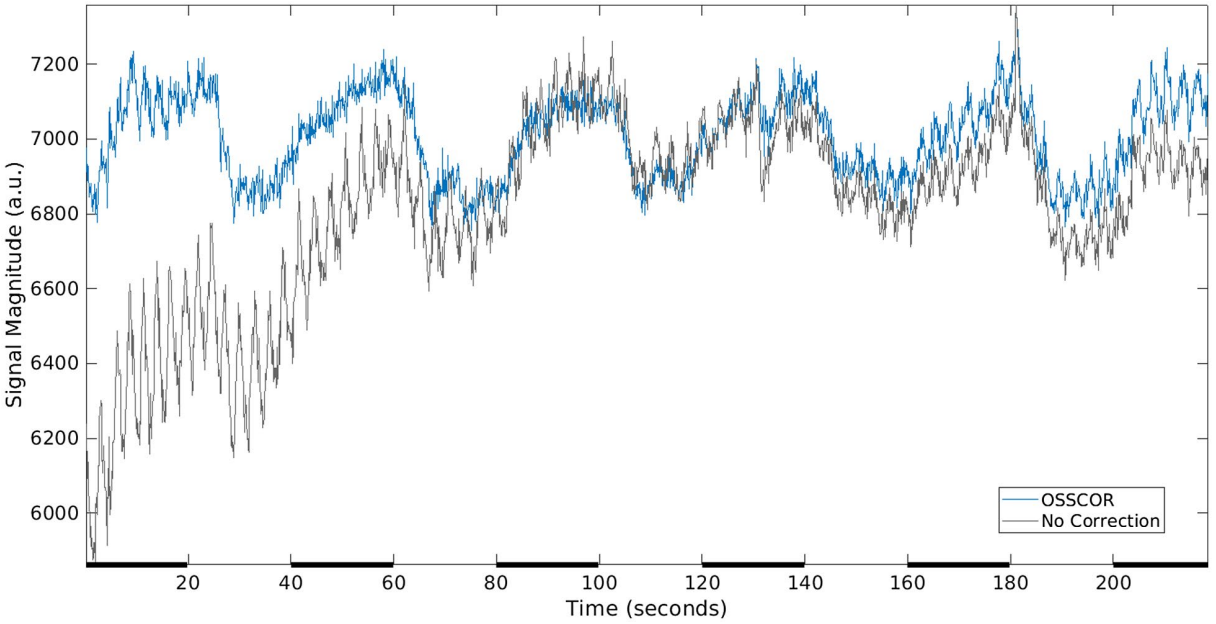

FIGURE 4 An example of uncorrected and OSSCOR-corrected phase timecourses, with the visual task indicated by black bars on the *x* axis. Although the uncorrected timecourse shows high sensitivity to respiration changes in the first minute of the scan, the OSSCOR method is able to regress out these physiological effects

implies that a sufficient range of off-resonant signals needs to be included in the analysis and that only selecting timecourses with high tSD results in a limited range of off-resonant behaviors represented in the nuisance regressors.

Our implementation of CompCor excluded timecourses that were correlated with the task above a threshold, although this preprocessing step was found to be unimportant for analyzing OSSI data. This result was confirmed by manually inspecting the unmodified tSD-derived ROI, which did not include voxels near the activated regions of the visual cortex. This preprocessing step was tested with OSSCOR to exclude phase timecourses potentially containing functional signal but was also found to have a negligible impact. Preprocessing the data using second-order polynomial detrending was effective at removing slowly varying noise components attributed to drift. This detrending step was found to be essential for defining the CompCor noise ROI based on tSD because respiration-induced noise magnitude is small compared to drift. However, the detrending step had a negligible effect on OSSCOR because no ROI is used, and low-frequency components are captured in the principal components. Although not necessary, polynomial detrending terms were included in OSSCOR and F-OSSCOR in order to match the degrees of freedom in method comparisons.

Whereas OSSCOR and F-OSSCOR demonstrate the ability to mitigate the effects of respiratory and scanner drift-induced frequency changes in OSSI, both methods inherit limitations of data-driven correction approaches. The first is the selection of how many principal components should be included in the analysis. Here, we have shown a rank can be selected through simulation; however, this does not account for subject-specific B_0 distributions or temporally varying respiration rates. This can lead to a deterioration of performance for some frequencies, as shown in the last 2 stimulus blocks in Figure 4, where no respiration artifacts are removed. Furthermore, flow-related artifacts in OSSI result in complex frequency-dependent signal evolutions, which were not well corrected by either proposed methods or CompCor. This effect can be seen in Figure 2, where tSNR did not improve in areas with significant vascular components.

Including all timecourses in OSSCOR creates the possibility of the nuisance regressors representing functional signal instead of noise, which would result in decreased functional sensitivity. This is of concern in the event of widespread activation or in cases in which there is no predefined task activity, such as in resting-state fMRI. For OSSCOR, such an issue may potentially be addressed through a CompCor-like strategy in which only white matter and CSF voxels are used as inputs. It is possible that F-OSSCOR would be less sensitive to the loss of resting-state activity since F-OSSCOR uses FID timecourses instead of voxel timecourses. This notion is supported by Figure 3B, where increasing the number of F-OSSCOR PCs did not appear to increase the number of false positives at the threshold used. Either of these modifications could be combined with common preprocessing steps such as band-pass filtering to exclude resting-state frequencies prior to applying PCA.

5 | CONCLUSION

We have shown that the application of OSSCOR and F-OSSCOR can significantly reduce physiological noise due to temporally varying off-resonance during an OSSI-based

fMRI acquisition. Unlike the previous PCA-based methods such as CompCor, OSSCOR does not require the selection of a designated noise ROI and instead uses OSSI-specific signal properties to determine correlated physiological noise components. Similarly, we show through F-OSSCOR that FID samples can be used to produce nuisance regressors independent of the image encoding strategy.

ACKNOWLEDGMENT

This work was supported by National Institute of Biomedical Imaging and Bioengineering (NIBIB) and National Institute of Neurological Disorders and Stroke (NINDS) through grants R01 EB023618 and U01 EB026977. We thank Dr. David Hong and Shouchang Guo for their discussions on signal modeling, which were immensely helpful in developing the methodology.

ORCID

Amos A. Cao https://orcid.org/0000-0003-0465-7053
Douglas C. Noll https://orcid.org/0000-0002-0983-3805

REFERENCES

1. Guo S, Noll DC. Oscillating steady-state imaging (OSSI): A novel method for functional MRI. *Magn Reson Med*. 2020;84:698-712.
2. Noll DC, Schneider W. Theory, simulation, and compensation of physiological motion artifacts in functional MRI. In Proceedings—International Conference on Image Processing (ICIP), Austin, TX, 1994. p. 40-44.
3. VanGelderen P, de Zwart J, Starewicz P, Hinks R, Duyn J. Real-time shimming to compensate for respiration-induced B0 fluctuations. *Magn Reson Med*. 2007;57:362-368.
4. Van de Moortele PF, Pfeuffer J, Glover GH, Ugurbil K, Hu X. Respiration-induced B0 fluctuations and their spatial distribution in the human brain at 7 Tesla. *Magn Reson Med*. 2002;47:888-895.
5. Lee J, Santos JM, Conolly SM, Miller KL, Hargreaves BA, Pauly JM. Respiration-induced B0 field fluctuation compensation in balanced SSFP: Real-time approach for transition-band SSFP fMRI. *Magn Reson Med*. 2006;55:1197-1201.
6. Glover GH, Li TQ, Ress D. Image-based method for retrospective correction of physiological motion effects in fMRI: RETROICOR. *Magn Reson Med*. 2000;44:162-167.
7. Thomas CG, Harshman RA, Menon RS. Noise reduction in BOLD-based fMRI using component analysis. *Neuroimage*. 2002;17:1521-1537.
8. Behzadi Y, Restom K, Liau J, Liu TT. A component-based noise correction method (CompCor) for BOLD and perfusion based fMRI. *Neuroimage*. 2007;37:90-101.
9. Perlbarg V, Bellec P, Anton JL, Pélégrini-Issac M, Doyon J, Benali H. CORSICA: Correction of structured noise in fMRI by automatic identification of ICA components. *Magn Reson Imaging*. 2007;25:35-46.
10. Churchill NW, Strother SC. PHYCAA+: An optimized, adaptive procedure for measuring and controlling physiological noise in BOLD fMRI. *Neuroimage*. 2013;82:306-325.
11. Nielsen JF, Noll DC. TOPPE: A framework for rapid prototyping of MR pulse sequences. *Magn Reson Med*. 2018;79:3128-3134.
12. Adolf D, Weston S, Baecke S, Luchtmann M, Bernarding J, Kropf S. Increasing the reliability of data analysis of functional magnetic resonance imaging by applying a new blockwise permutation method. *Front Neuroinform*. 2014;8:72.

SUPPORTING INFORMATION

Additional Supporting Information may be found online in the Supporting Information section.

FIGURE S1 Individual OSSCOR nuisance regressors plotted for k = 6. Each principal component can be seen to contain low frequency components due to drift effects, as well as high frequency components due to respiration. Note that while each of the 6 regressors contains fluctuations due to respiration, the phase of the fluctuations varies between regressors

FIGURE S2 Scree plots for simulated physiological noise (A), as well as OSSCOR (B) and F-OSSCOR (C) applied to $n = 6$ subject scans. In the experimental data, the plots show that energy of the PCs is reduced by slightly reduced amount for OSSCOR and a similar amount for F-OSSCOR, in comparison to the simulated physiological noise

FIGURE S3 Activation maps for all $n = 6$ subjects computed for each denoising approach using a random blockwise permutation analysis, thresholded at $P = .001$. Each analysis used 1,000,000 permutations of 10 timecourse blocks, with random circular shifts added before block randomization. Masks for each subject are shown, indicating voxel regions that were counted as true activation. See "Data Analysis" for a description of how true and false activation regions were estimated

TABLE S1 Summary of permutation test results, showing the number of true and false activated voxels from the activation maps and masks shown in Supporting Information Figure S3

How to cite this article: Cao AA, Noll DC. A retrospective physiological noise correction method for oscillating steady-state imaging. *Magn Reson Med*. 2021;85:936–944. https://doi.org/10.1002/mrm.28414